

MagiNet: Mask-Aware Graph Imputation Network for Incomplete Traffic Data

JIANPING ZHOU, Shanghai Jiao Tong University, China

BIN LU, Shanghai Jiao Tong University, China

ZHANYU LIU, Shanghai Jiao Tong University, China

SIYU PAN, Shanghai Jiao Tong University, China

XUEJUN FENG, Shanghai Jiao Tong University, China

HUA WEI, Arizona State University, USA

GUANJIE ZHENG, Shanghai Jiao Tong University, China

XINBING WANG, Shanghai Jiao Tong University, China

CHENGHU ZHOU, Chinese Academy of Sciences, China

Due to detector malfunctions and communication failures, missing data is ubiquitous during the collection of traffic data. Therefore, it is of vital importance to impute the missing values to facilitate data analysis and decision-making for Intelligent Transportation System (ITS). However, existing imputation methods generally perform *zero* pre-filling techniques to initialize missing values, introducing inevitable noises. Moreover, we observe prevalent over-smoothing interpolations, falling short in revealing the intrinsic spatio-temporal correlations of incomplete traffic data. To this end, we propose *Mask-aware graph imputation Network*: **MagiNet**. Our method designs an adaptive mask spatio-temporal encoder to learn the latent representations of incomplete data, eliminating the reliance on pre-filling missing values. Furthermore, we devise a spatio-temporal decoder that stacks multiple blocks to capture the inherent spatial and temporal dependencies within incomplete traffic data, alleviating over-smoothing imputation. Extensive experiments demonstrate that our method outperforms state-of-the-art imputation methods on five real-world traffic datasets, yielding an average improvement of 4.31% in RMSE and 3.72% in MAPE.

CCS Concepts: • **Computing methodologies** → **Artificial intelligence**; **Spatio-temporal Data**.

Additional Key Words and Phrases: Traffic Data Imputation, Graph Neural Network

ACM Reference Format:

Jianping Zhou, Bin Lu, Zhanyu Liu, Siyu Pan, Xuejun Feng, Hua Wei, Guanjie Zheng, Xinbing Wang, and Chenghu Zhou. 2018. MagiNet: Mask-Aware Graph Imputation Network for Incomplete Traffic Data. *J. ACM* 37, 4, Article 111 (August 2018), 19 pages. <https://doi.org/XXXXXXXX.XXXXXXX>

Authors' addresses: Jianping Zhou, jianpingzhou@sjtu.edu.cn, Shanghai Jiao Tong University, Shanghai, China; Bin Lu, robinlu1209@sjtu.edu.cn, Shanghai Jiao Tong University, Shanghai, China; Zhanyu Liu, zhyluu00@sjtu.edu.cn, Shanghai Jiao Tong University, Shanghai, China; Siyu Pan, pansiyu0327@sjtu.edu.cn, Shanghai Jiao Tong University, Shanghai, China; Xuejun Feng, fengxuejun@sjtu.edu.cn, Shanghai Jiao Tong University, Shanghai, China; Hua Wei, hua.wei@asu.edu, Arizona State University, Arizona, USA; Guanjie Zheng, Shanghai Jiao Tong University, Shanghai, China, gjzheng@sjtu.edu.cn; Xinbing Wang, Shanghai Jiao Tong University, Shanghai, China, xwang8@sjtu.edu.cn; Chenghu Zhou, Chinese Academy of Sciences, Beijing, China, zhouchsjtu@gmail.com.

Permission to make digital or hard copies of all or part of this work for personal or classroom use is granted without fee provided that copies are not made or distributed for profit or commercial advantage and that copies bear this notice and the full citation on the first page. Copyrights for components of this work owned by others than the author(s) must be honored. Abstracting with credit is permitted. To copy otherwise, or republish, to post on servers or to redistribute to lists, requires prior specific permission and/or a fee. Request permissions from permissions@acm.org.

© 2018 Copyright held by the owner/author(s). Publication rights licensed to ACM.

ACM 0004-5411/2018/8-ART111

<https://doi.org/XXXXXXXX.XXXXXXX>

1 INTRODUCTION

Missing data problems are pervasive when collecting traffic data from the Intelligent Transportation System (ITS) [37, 41, 45, 46], owing to numerous uncontrollable factors, such as detector malfunctions, communication failures, and maintenance issues [5, 24, 29, 35]. Incomplete traffic data hinders comprehensive data analysis and decision-making. Consequently, how to impute the missing values in traffic data arises as an important problem.

The first and foremost issue lies in the initialization of missing values. Specifically, how to replace the missing value placeholder, i.e., *NaN*, for feature extraction. Traditional statistical methods [13, 33, 38] do not initialize missing values. Instead, they directly impute missing values utilizing the statistical indicators of available observations. These approaches rely on the strong assumption of time series stationarity, which fails to capture the nonlinear properties in incomplete traffic data, leading to poor performance. Recent deep imputation methods [1, 3, 40, 43] primarily employ *zero pre-filling* to initialize missing values and use a mask matrix to record their positions. The incomplete data is then treated as *complete* data to ensure spatio-temporal feature learning. However, utilizing pre-filling techniques to initialize missing values inevitably introduces noise and misleads the feature learning process. We present an example of incomplete traffic data from the Seattle dataset for a single day in Figure 1(a). Subsequently, we compare the imputation performance with and without pre-filling missing values. As shown in Figure 1(b), the imputation performance with pre-filling missing values is significantly worse than without pre-filling.

Another issue is capturing the spatial and temporal correlations within incomplete traffic data. To be specific, how to aggregate observation information to impute missing values while avoiding the over-smoothing effect. Many traffic forecasting methods [14, 16, 31, 39, 44] have conducted research on capturing spatio-temporal dependencies, but they rely on complete history data, rendering them unsuitable for missing scenarios. Moreover, most imputation methods [3, 27, 43] do not simultaneously consider the complex spatial and temporal dependencies. Recent deep models tailored for spatio-temporal imputation, such as GRIN [1] and GA-GAN [40], utilize pre-filled data to capture spatio-temporal correlations. However, these approaches ignore inherent dynamic changes, resulting in an over-smoothing effect, as shown in Figure 1(c).

Therefore, to address the above two issues, we propose *Mask-aware graph imputation Network* in an encoder-decoder framework, named **MagiNet**. The core idea of our method is to adaptively learn the representation of missing values and capture intrinsic spatio-temporal correlations within incomplete data. Firstly, we propose an adaptive mask spatio-temporal encoder (*AMSTenc*) that generates representations of missing values through a learnable missing encoding, which adaptively learns inherent representations without introducing supplementary noise. Additionally, we utilize a mask-aware spatio-temporal decoder (*MASTdec*) that stacks multiple blocks, adopting a mask-aware attention mechanism. The decoder incorporates the adaptive missing embedding to consciously adjust the aggregation coefficient with observation embedding, extracting inherent correlations within incomplete traffic data and alleviating the over-smoothing effect.

In summary, the main contributions are as follows:

- We design an adaptive mask spatio-temporal encoder that does not require pre-filling techniques. It dynamically learns the representation of incomplete traffic data, effectively eliminating the introduction of uncontrollable noise.
- We design a spatio-temporal decoder that incorporates a mask-aware attention mechanism to capture inherent dependencies within incomplete data and alleviate the over-smoothing effect.
- Experimental results on five real-world traffic datasets show that our method outperforms state-of-the-art imputation methods, with an average improvement of 4.31% in RMSE and 3.72% in MAPE, and consistently exhibits improvement across different missing ratios.

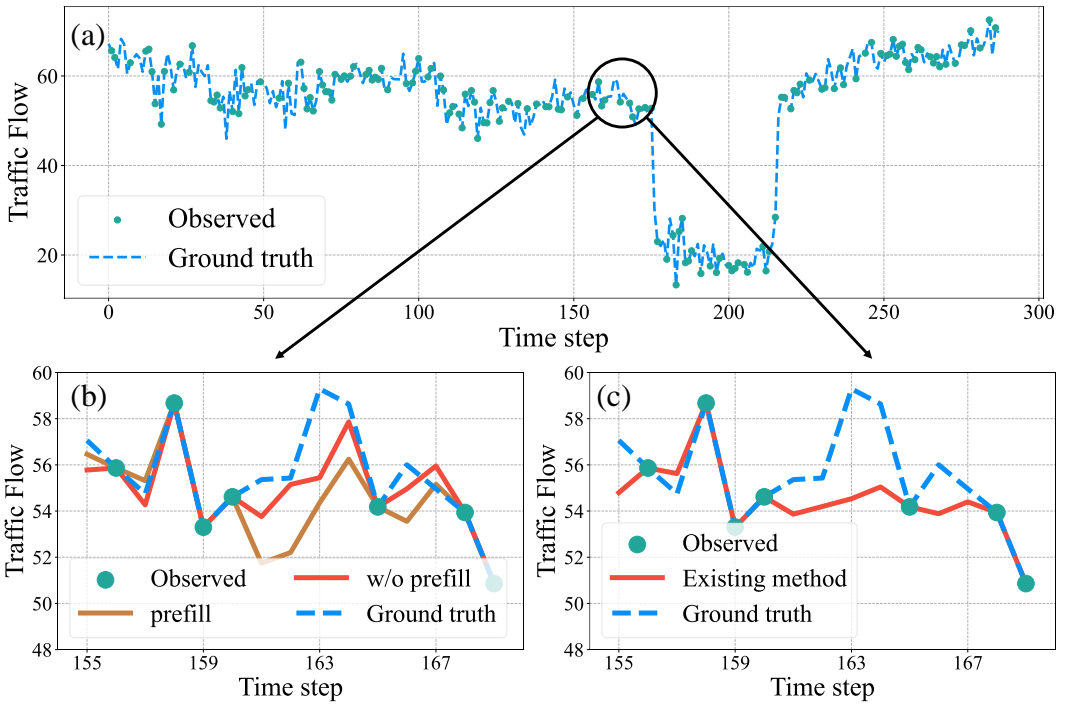


Fig. 1. (a) Example of incomplete traffic data and corresponding ground truth from the Seattle dataset. (b) Performance comparison with and without pre-filling techniques to initialize missing values. Imputation performance with pre-filling techniques is significantly worse than without pre-filling. (c) Existing methods fail to capture inherent spatio-temporal correlations in incomplete traffic data, leading to an over-smoothing effect at dynamic missing positions, particularly noticeable between time steps 160 and 168.

2 RELATED WORK

2.1 Missing Data Imputation

Existing methods for missing data imputation could be generally divided into three categories: *statistical learning-based methods*, *machine learning-based methods*, and *deep learning-based methods*. (1) The *statistical learning-based methods*, such as Mean, Median, KNN [33], and MICE [38], impute missing values based on the statistical properties of the available observations, assuming the time series is stationary. However, they fail to capture the nonlinear characteristics inherent in incomplete traffic data. (2) The *machine learning-based methods* include the traditional probabilistic principal component analysis [26], matrix factorization [4, 9, 10] and EM algorithms [22]. However, these methods cannot simultaneously learn the dynamic spatio-temporal correlations, and the computational complexity increases significantly when handling high-dimensional data. (3) Recently, a plethora of *deep learning-based methods* have been proposed. BRITS [3] utilizes the bidirectional recurrent neural network architecture to capture temporal features. MIWAE [21], GAIN [43], MISGAN [15], Mcflow [27], ST-SCL [25] treat the imputation task as the temporal generation task, incorporating popular generative architectures, such as AutoEncoder [12], GAN [6], and Flow [11]. However, traffic data is a type of data with temporal and spatial characteristics, and obviously, these methods ignore the modeling of spatial features. GRIN [1], GA-GAN [40] involve graph neural networks to capture spatial correlations, but these methods utilize pre-filling

techniques to initialize missing values, introducing supplementary noises. PriSTI [18] employs MPNN and diffusion modules to extract features, but its message-passing mechanism falls short in capturing inherent spatio-temporal correlation within incomplete traffic data.

2.2 Modeling the Spatio-temporal Dependency

In recent years, numerous deep models tailored for spatio-temporal data have been developed to capture spatial and temporal dependencies, such as STGCN [44], DCRNN [16], Graph WaveNet [39], and others [2, 8, 14, 31, 36, 42]. These methods design diverse graph convolution modules to extract spatio-temporal features for traffic forecasting task, where the primary objective is to predict future traffic data by leveraging complete history data. However, in the real world, the missing data problem is pervasive in traffic data, preventing these methods from accessing complete traffic data to capture spatio-temporal dependencies. In this paper, our task concentrates on imputing missing values based on observations from the incomplete data, rather than utilizing complete history data to forecast future data. Therefore, we need to address how to capture inherent spatio-temporal dependencies within incomplete traffic data instead of complete data.

3 PRELIMINARY

In this section, we first define the concept of incomplete traffic data and then give the problem definition of imputation task.

DEFINITION 1. *Due to real-world detectors commonly manifest a non-uniform spatial distribution, we define the incomplete traffic data as graph-based data $\mathcal{D} = \{\mathcal{G}, (\mathbf{X}_t, \mathbf{M}_t)_{t=1}^T\}$, spanning T time steps. \mathcal{G} denotes the underlying traffic network, actually $\mathcal{G} = (\mathcal{V}, \mathcal{E}, \mathbf{A})$, where \mathcal{V} is a finite set of $|\mathcal{V}| = N$ nodes, \mathcal{E} is a set of connecting edges between nodes in \mathcal{V} , and \mathbf{A} is the adjacency matrix of \mathcal{G} . $\mathbf{X}_t = (\mathbf{x}_t^1, \mathbf{x}_t^2, \dots, \mathbf{x}_t^N) \in \mathbb{R}^{N \times C}$ denotes the incomplete values of all nodes at the timestamp t , where $\mathbf{x}_t^i \in \mathbb{R}^C$ denotes the incomplete values of C features of node i at the timestamp t . $\mathbf{M}_t = (m_t^1, m_t^2, \dots, m_t^N) \in \{0, 1\}^N$ is the mask matrix. $m_t^i \in \{0, 1\}$ denotes whether the \mathbf{x}_t^i is observed: 1 indicates \mathbf{x}_t^i is observed, and 0 indicates \mathbf{x}_t^i is missing.*

PROBLEM 1. Incomplete Traffic Data Imputation. *Suppose we have incomplete traffic data over τ time slices, and we want to impute the missing values. The imputation task is formulated as learning a function $f(\cdot)$ given a underlying graph \mathcal{G} :*

$$[(\mathbf{X}_1, \mathbf{M}_1), \dots, (\mathbf{X}_\tau, \mathbf{M}_\tau); \mathcal{G}] \xrightarrow{f(\cdot)} [\hat{\mathbf{X}}_1, \dots, \hat{\mathbf{X}}_\tau], \quad (1)$$

such that minimizes the estimation error on missing positions, where $\hat{\mathbf{X}}_t \in \mathbb{R}^{N \times C}$ denotes the imputed data at the timestamp t .

In this paper, all the notation is summarized in Table 1 for brevity.

4 METHODOLOGY

In this section, we introduce our model, MagiNet, to tackle the incomplete traffic data imputation task. The proposed MagiNet, shown in Figure 2, includes an adaptive mask spatio-temporal encoder (*AMSTenc*) and a mask-aware spatio-temporal decoder (*MASTdec*). Firstly, the incomplete traffic data is fed into the encoder to generate an adaptive representation, which is subsequently transmitted to the decoder. The decoder stacks multiple blocks incorporating a mask-aware spatio-temporal attention mechanism (*MASTatt*) and attention-based spatio-temporal aggregation to capture inherent dependencies within incomplete data. Finally, the missing values are imputed utilizing the information from correlated observations. The specific details are discussed in the following parts.

Table 1. Notations.

Notation	Definition	Notation	Definition
\mathcal{D}	incomplete traffic dataset	X_o	the observation embedding
\mathcal{G}	the underlying traffic graph	Z_u	the learnable missing embedding
\mathcal{V}	the node set of \mathcal{G}	X_p	the incomplete traffic data embedding
\mathcal{E}	the edge set of \mathcal{G}	H	the latent representation after <i>AMSTenc</i>
A	the adjacency matrix of \mathcal{G}	T_{att}	the mask-aware temporal attention score
X_t	the incomplete traffic data at timestamp t	$A^{(l)}$	the temporal attention score of the l -th block
M_t	the mask matrix of X_t	H_{matt}	the representation after temporal attention aggregation
\hat{X}_t	the imputed traffic data	H'_{matt}	the representation after spatial attention aggregation
$f(\cdot)$	the function to impute the missing values	S_{att}	the spatial attention score
N	the number of nodes	E	the representation after graph convolution
T	the length of time steps	E_{out}	the representation after multi-scale temporal convolution
C	the number of features	H_{out}	the output of mask-aware spatio-temporal block

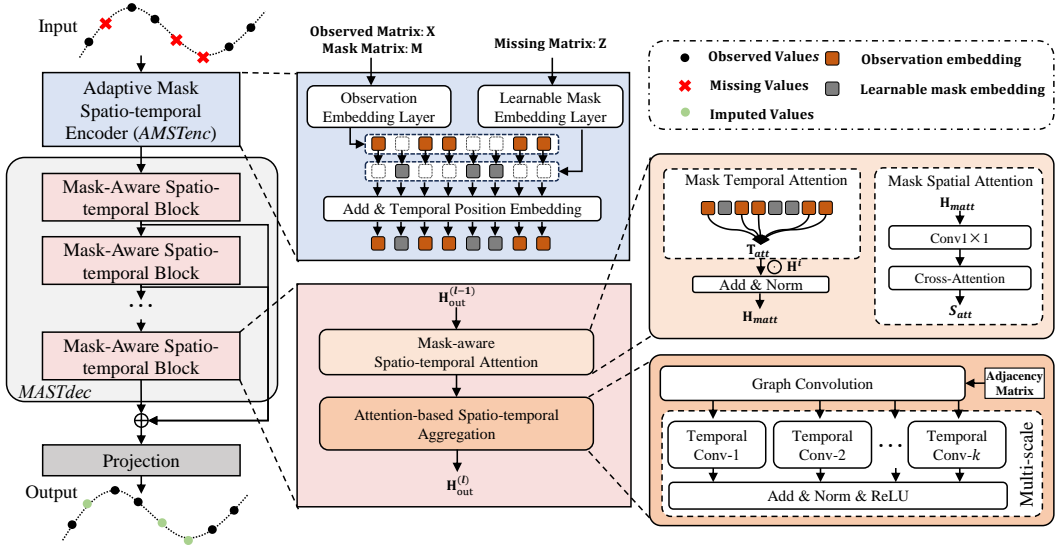


Fig. 2. An overview of MagiNet, which consists of an adaptive mask spatio-temporal encoder (*AMSTenc*) and a mask-aware spatio-temporal decoder (*MASTdec*). The *MASTdec* stacks several spatio-temporal blocks (*ST Block*). Each *ST Block* combines a mask-aware spatio-temporal attention (*MASTatt*) module that calculates the mask temporal and spatial attention, an attention-based spatio-temporal aggregation module that aggregates spatial information using graph convolution and multi-scale temporal information using temporal convolution.

4.1 Adaptive Mask Spatio-temporal Encoder

In this part, we discuss how to accurately represent incomplete traffic data without resorting to pre-filling techniques. We claim that the incomplete traffic data is decomposed into a feature matrix $X \in \mathbb{R}^{N \times T \times C}$, a mask matrix $M \in \{0, 1\}^{N \times T}$, and a missing matrix $Z \in \mathbb{R}^{N \times T \times C}$. X records the observed values, M records the missing positions, and Z represents the missing values. We propose an adaptive mask spatio-temporal encoder (*AMSTenc*), which can adaptively represent missing values without initializing missing values with zero.

First, we encode the feature matrix \mathbf{X} to obtain the representations of observed features $\mathbf{X}_o \in \mathbb{R}^{N \times T \times d}$ through an observation embedding layer, which is denoted as follows:

$$\mathbf{X}_o = \mathbf{X} \cdot \mathbf{W}_o + \mathbf{b}_o, \quad (2)$$

where $\mathbf{W}_o \in \mathbb{R}^{C \times d}$, $\mathbf{b}_o \in \mathbb{R}^d$ are trainable parameters, d is the size of hidden dimension. Meanwhile, we use a learnable mask embedding layer to acquire representations $\mathbf{Z}_u \in \mathbb{R}^{N \times T \times d}$ of the missing matrix \mathbf{Z} . Then, we extract the representations of the observed segment in \mathbf{X}_o and the learnable representations of the missing segment in \mathbf{Z}_u . We combine the extracted representations to yield the incomplete data representations $\mathbf{X}_p \in \mathbb{R}^{N \times T \times d}$:

$$\mathbf{X}_p = \mathbf{X}_o \odot \mathbf{M} + \mathbf{Z}_u \odot (\mathbf{1} - \mathbf{M}), \quad (3)$$

where we broadcast \mathbf{M} to the same dimension as \mathbf{X}_o , \odot is the Hadamard product. Next, we integrate a temporal positional embedding layer to add temporal sequence information. Note that the temporal positional embedding is a learnable embedding rather than the sinusoidal embedding [30]. Finally, we obtain the latent representations $\mathbf{H} \in \mathbb{R}^{N \times T \times d}$.

4.2 Mask-Aware Spatio-temporal Decoder

In this part, we discuss how to effectively capture inherent spatio-temporal dependencies within incomplete data. Previous methods [14, 16, 31, 39, 44] rely on complete data to capture spatio-temporal dependencies, making them unsuitable for scenarios with missing data. Spatio-temporal imputation methods such as GRIN [1] and GA-GAN [40] utilize pre-filled data to capture spatio-temporal correlations, resulting in over-smoothing at dynamic missing positions. To address these limitations, we propose a mask-aware spatio-temporal decoder (*MASTdec*) that stacks multiple blocks to capture intrinsic spatio-temporal dependencies within the latent representations \mathbf{H} obtained through the *AMSTenc*. In each block of *MASTdec*, we adopt a mask-aware spatio-temporal attention mechanism to assess the importance of distinct nodes. Then, we utilize a spatial convolution based on this attention mechanism to enable the comprehensive aggregation of spatio-temporal information from diverse nodes. Moreover, we incorporate a multi-scale temporal convolution to update the information attributed to each node.

4.2.1 Mask-Aware Spatio-temporal Attention.

We design a mask-aware spatio-temporal attention mechanism (*MAStatt*) to capture inherent correlations within incomplete data. First, we utilize a multi-head self-attention [34] incorporating a mask-aware mechanism to capture intricate temporal dependencies between nodes. For the multi-head attention of m heads, we define the following variables:

$$\mathbf{Q}^{(h)} \triangleq \mathbf{H}\mathbf{W}_q^{(h)}, \mathbf{K}^{(h)} \triangleq \mathbf{H}\mathbf{W}_k^{(h)}, \mathbf{V}^{(h)} \triangleq \mathbf{H}\mathbf{W}_v^{(h)}, \quad (4)$$

$$\mathbf{T}_{att} = [\mathbf{T}_{att}^{(1)}, \mathbf{T}_{att}^{(2)}, \dots, \mathbf{T}_{att}^{(m)}], \text{ where } \mathbf{T}_{att}^{(h)} = \frac{\mathbf{Q}^{(h)}\mathbf{K}^{(h)\top}}{\sqrt{d_h}}, \quad (5)$$

$$\mathbf{A}^{(l)} = \mathbf{T}_{att} + \mathbf{A}^{(l-1)}, \quad (6)$$

where $\mathbf{W}_q^{(h)}, \mathbf{W}_k^{(h)}, \mathbf{W}_v^{(h)} \in \mathbb{R}^{d \times d_h}$ are the h -th head parameters, $\mathbf{Q}^{(h)}, \mathbf{K}^{(h)}, \mathbf{V}^{(h)} \in \mathbb{R}^{N \times T \times d_h}$, $h = 1, 2, \dots, m$, and d_h represents the size of the hidden dimension. Then, the attention score $\mathbf{T}_{att} \in \mathbb{R}^{N \times m \times T \times T}$ is derived by Eq (5). We employ the attention residual connection to augment the interconnection among the mask temporal attention across multiple spatio-temporal blocks on Eq (6), where $\mathbf{A}^{(l)} \in \mathbb{R}^{N \times m \times T \times T}$ represents the temporal attention of the l -th spatio-temporal block,

$\mathbf{A}^{(0)} = 0$. To ignore the impact of missing values on observations, we multiply the mask matrix \mathbf{M} to get the mask-aware attention context $\mathbf{C} \in \mathbb{R}^{N \times m \times T \times d_h}$:

$$\mathbf{C} = \text{Softmax}(\mathbf{M} \odot \mathbf{A}^{(l)}) \mathbf{V}^{(l)}, \quad (7)$$

$$\mathbf{H}_{\text{matt}} = \text{LN}((\mathbf{C} \cdot \mathbf{W}_c + \mathbf{b}_c) + \mathbf{H}). \quad (8)$$

We reshape the \mathbf{C} , and subsequently feed to a linear layer and a residual connection with \mathbf{H} . Then the output $\mathbf{H}_{\text{matt}} \in \mathbb{R}^{N \times T \times d}$ is obtained through a normalization layer, computed as Eq (8), where $\text{LN}(\cdot)$ represents the layer normalization, $\mathbf{W}_c \in \mathbb{R}^{m \times d_h \times d}$, $\mathbf{b}_c \in \mathbb{R}^d$ are trainable parameters. After that, we utilize a 1D convolution to aggregate the temporal representations of \mathbf{H}_{matt} , and then add spatial position information to obtain a high-dimensional latent representation $\mathbf{H}'_{\text{matt}} \in \mathbb{R}^{N \times F}$ of each node, where F is the dimension of spatial node embedding. We project $\mathbf{H}'_{\text{matt}}$ into two branches, and then calculate the mask-aware spatial attention as follows:

$$\mathbf{Q}'^{(h)} \triangleq \mathbf{H}'_{\text{matt}} \mathbf{W}'_q{}^{(h)}, \quad \mathbf{K}'^{(h)} \triangleq \mathbf{H}'_{\text{matt}} \mathbf{W}'_k{}^{(h)}, \quad (9)$$

$$\mathbf{S}_{\text{att}}^{(h)} = \text{Softmax}\left(\frac{\mathbf{Q}'^{(h)} \mathbf{K}'^{(h)T}}{\sqrt{d_h}}\right), \quad (10)$$

$$\mathbf{S}_{\text{att}} = [\mathbf{S}_{\text{att}}^{(1)}, \mathbf{S}_{\text{att}}^{(2)}, \dots, \mathbf{S}_{\text{att}}^{(m)}], \quad (11)$$

where $\mathbf{W}'_q{}^{(h)}, \mathbf{W}'_k{}^{(h)} \in \mathbb{R}^{F \times d_h}$ are the h -th head parameters, and $\mathbf{Q}'^{(h)}, \mathbf{K}'^{(h)} \in \mathbb{R}^{N \times d_h}$, $h = 1, 2, \dots, m$. Finally, we concatenate the spatial attention of m heads to represent the mask-aware spatio-temporal attention $\mathbf{S}_{\text{att}} \in \mathbb{R}^{m \times N \times N}$.

4.2.2 Attention-based Spatio-temporal Aggregation.

In order to further aggregate spatio-temporal features of neighboring nodes, we design an attention-based spatio-temporal aggregation module. Unlike previous methods [16, 44] directly aggregate the spatio-temporal features of neighboring nodes based on traffic road network in graph convolution, the mask-aware attention strategy aims to consciously adjust the aggregation. To be specific, the information aggregated during graph convolution is the adaptive mask spatio-temporal representation \mathbf{H} and the mask-aware spatio-temporal attention \mathbf{S}_{att} is used as weights. After that, the multi-scale temporal information is aggregated using multiple temporal convolutions with diverse kernel sizes.

Regarding the graph convolution, we adopt Chebyshev polynomial approximation [32] to learn structure-aware node features. The laplacian matrix for Chebyshev polynomial is defined as $\mathbf{L} = \mathbf{D} - \mathbf{A}$, and its normalized form is $\tilde{\mathbf{L}} = \frac{2}{\lambda_{\max}} (\mathbf{D} - \mathbf{A}) - \mathbf{I}_N \in \mathbb{R}^{N \times N}$, where \mathbf{A} is the adjacency matrix, \mathbf{I}_N is a unit matrix, $\mathbf{D} \in \mathbb{R}^{N \times N}$ is the degree matrix, $D_{ii} = \sum_j \mathbf{A}_{ij}$, and λ_{\max} is the maximum eigenvalue of the Laplacian matrix \mathbf{L} .

Then, we utilize the K -th order Chebyshev polynomials T_k to aggregate the information between nodes, which is calculated as follows:

$$g_\theta *_G x = g_\theta(\mathbf{L})x = \sum_{k=0}^{K-1} \theta_k (T_k(\tilde{\mathbf{L}}) \odot \mathbf{S}_{\text{att}}^{(k)})x. \quad (12)$$

Here, we let the graph signal at each time is $x = \mathbf{x}_t \in \mathbb{R}^{N \times C}$. g_θ denotes the approximate convolution kernel, $*_G$ denotes the graph convolution operation, and $\theta \in \mathbb{R}^K$ is the convolution kernel parameter. Note that we accompany $T_k(\tilde{\mathbf{L}})$ with the mask-aware spatio-temporal attention $\mathbf{S}_{\text{att}}^{(k)}$, which can dynamically adapt the information aggregation in the context of incomplete data.

After the mask-aware spatial convolution updates the spatio-temporal features of each node, we subsequently proceed to update the information corresponding to each time point. We utilize

the gated temporal convolution layer [14, 39] to aggregate temporal features, thereby propagating information from observed time points to missing time points.

We denote the output of Chebyshev graph convolution as $\mathbf{E}^{(l)} \in \mathbb{R}^{N \times T \times d}$ in the l -th block. To simplify the notation, we drop the superscript l . Then, \mathbf{E} is fed into k gated temporal convolution blocks, where each block applies a 1D convolution kernel $\Gamma \in \mathbb{R}^{1 \times K \times d \times 2d}$ with a size of $1 \times K$, followed by two branches involving *sigmoid* and *tanh* operations. The gated temporal convolution operation can be defined as:

$$\Gamma *_y \mathbf{E} = \phi(\mathbf{E}) \odot \sigma(\mathbf{E}), \quad (13)$$

where $*_y$ is gated temporal convolution operator, $\phi(\cdot)$ is the *tanh* function, and $\sigma(\cdot)$ is the *sigmoid* function. The outputs of multiple gated temporal convolutions are concatenated, followed by an add operation with \mathbf{E} , and then passed through a ReLU activation function. The output $\mathbf{E}_{out} \in \mathbb{R}^{N \times T \times d}$, is derived by Eq (14), where $\Gamma_1, \dots, \Gamma_k$ are convolution kernels with size K_1, \dots, K_k , \parallel is concatenation.

$$\mathbf{E}_{out} = \text{ReLU}((\Gamma_1 *_y \mathbf{E} \parallel \Gamma_2 *_y \mathbf{E} \cdots \parallel \Gamma_k *_y \mathbf{E}) + \mathbf{E}), \quad (14)$$

$$\mathbf{H}_{out} = \text{LN}(\text{ReLU}(\mathbf{E}_{out} \parallel \mathbf{H})). \quad (15)$$

Finally, to alleviate gradient dispersion, \mathbf{E}_{out} is combined with \mathbf{H} through a residual connection, a ReLU activation function, and a layer normalization to obtain the output $\mathbf{H}_{out} \in \mathbb{R}^{N \times T \times d}$.

4.3 Projection Layer

Assume the *MASTdec* stacks L layers of spatio-temporal blocks, we concatenate the output from each block. Then, we utilize a two-layer fully connected network, i.e., FC, as a output layer and apply the concatenated output to acquire imputation results $\hat{\mathbf{X}} \in \mathbb{R}^{N \times T \times C}$:

$$\hat{\mathbf{X}} = \text{FC}\left(\sum_{i=1}^L \mathbf{H}_{out}^{(i)}\right). \quad (16)$$

4.4 Training Strategy

Given the ground truth $\tilde{\mathbf{X}} \in \mathbb{R}^{N \times \tau \times C}$ on missing positions over τ slices, we optimize our model using L1 loss:

$$\mathcal{L}(\hat{\mathbf{X}}, \tilde{\mathbf{X}}, \mathbf{M}) = \frac{1}{\tau} \sum_{t=1}^{\tau} \frac{\frac{1}{N} \sum_{i=1}^N \bar{m}_t^i \cdot \frac{1}{C} \sum_{j=1}^C |\hat{x}_{t,j}^i - \tilde{x}_{t,j}^i|}{\sum_{i=1}^N \bar{m}_t^i}, \quad (17)$$

where $\hat{x}_{t,j}^i, \tilde{x}_{t,j}^i$ are elements of $\hat{\mathbf{X}}, \tilde{\mathbf{X}}$, respectively. \bar{m}_t^i is the logical binary complement of m_t^i . The training pipeline is shown in Algorithm 1.

Algorithm 1: The Training Process of MagiNet.

Input: Incomplete traffic data: a feature matrix X , a mask matrix M and a missing matrix Z ;
The ground-truth of incomplete traffic data \tilde{X}

Output: The model parameter of optimized MagiNet θ

- 1 Random initialize θ ;
- 2 **for** e in range(0, epochs, 1) **do**
- 3 Obtain the observation embedding X_o by Eq (2);
- 4 Obtain the learnable missing embedding Z_u and then yield the representation of incomplete traffic data X_p by Eq (3);
- 5 Add the temporal positional embedding and then obtain the output H of *AMSTenc*;
 // there is L spatio-temporal blocks
- 6 **for** $l = 1$ to L **do**
- 7 Calculate the mask-aware spatio-temporal attention T_{att} and S_{att} by Eq (4) to Eq (11);
- 8 Carry out the attention-based spatio-temporal aggregation by Eq (12) to Eq (15);
- 9 Output the H_{out}^l of each block;
- 10 **end**
- 11 Concatenate each block's output and utilize a projection layer to obtain the imputation results \tilde{X} by Eq (16);
- 12 Compute the training loss \mathcal{L} by Eq (17);
- 13 Use $\nabla_{\theta} \mathcal{L}$ to update θ with Adam optimizer;
- 14 **end**
- 15 return θ

5 EXPERIMENTS

In this section, we conduct extensive experiments to verify the effectiveness of our model, MagiNet. Specifically, the following research questions are answered:

- **RQ1:** How does MagiNet perform compared to other baselines on different datasets?
- **RQ2:** What is the individual contribution of each component in MagiNet to its imputation performance?
- **RQ3:** How does MagiNet perform with respect to different missing ratios?
- **RQ4:** What is the impact of each major hyperparameter on MagiNet's performance?

5.1 Experimental Setup

5.1.1 Datasets. We evaluate our model MagiNet on five real-world traffic datasets: METR-LA, Seattle, Chengdu, Shenzhen, PEMS-BAY [20, 40].

- **METR-LA:** The traffic dataset is collected from loop-detectors located on the Los Angeles County road network. Specifically, METR-LA contains 4 months of data recorded by 207 traffic sensors from Mar 1st, 2012 to June 30th, 2012. The data collection interval is 5 minutes, and the total number of timesteps is 34,272.
- **Seattle:** The traffic dataset is collected in the Seattle area from 323 detectors throughout 2015. The data collection interval is 5 minutes, and the total number of timesteps is 105,120.
- **Chengdu:** Traffic index dataset of Chengdu, China, is provided by Didi Chuxing GAIA Initiative. Chengdu contains data from January to April 2018, with 524 roads in the core urban area of Chengdu. The data collection interval is 5 minutes, and the total number of timesteps is 17,280.

- **Shenzhen**: Traffic index dataset of Shenzhen, China, is provided by Didi Chuxing GAIA Initiative. Shenzhen contains data from January to April 2018, with 627 roads in downtown Shenzhen. The data collection interval is 5 minutes, and the total number of timesteps is 17,280.
- **PEMS-BAY**: The traffic dataset is collected from California Transportation Agencies (CalTrans) Performance Measurement System (PeMS). Specifically, PEMS-BAY contains 6 months of data recorded by 325 traffic sensors in the Bay Area from January 1st, 2017 to June 30th, 2017. The data collection interval is 5 minutes, and the total number of timesteps is 52,116.

Consistent with the experimental settings of previous works [19, 20, 30], we adopt the following data division strategies: For METR-LA, Seattle, and PEMS-BAY, we sample the datasets every 12 time steps. About 70% of the data is used for training, 20% for validation, and the remaining 10% for testing. For Chengdu and Shenzhen, we sample the datasets every 6 time steps. About 60% of the data is used for training, 20% for validation, and the remaining 20% for testing. The statistical information is summarized in Table 2.

Table 2. Statistics of traffic datasets.

Datasets	Nodes	Edges	Timesteps	Interval	#Train	#Valid	#Test	Mean	Std
METR-LA	207	1,722	34,272	5 min	1,999	285	571	54.274	19.664
Seattle	323	1,001	105,120	5 min	6,132	876	1,752	56.854	12.580
Chengdu	524	1,120	17,280	10 min	1,728	576	576	29.616	9.713
Shenzhen	627	4,845	17,280	10 min	1,728	576	576	31.066	11.126
PEMS-BAY	325	2,694	52,116	5 min	3,024	432	864	62.722	9.455

5.1.2 Baselines. We compare the proposed model, MagiNet, with the following baselines. Mean, KNN [33], MissForest [28], MF [13], and MICE [38] are traditional statistical learning-based or machine learning-based methods. To compare the capability of capturing spatio-temporal dependencies within incomplete traffic data, we select five widely used traffic forecasting methods that incorporate pre-filling techniques to address the imputation task: STGCN [44], DCRNN [16], GWNet [39], DSTAGNN [14], D2STGNN [31]. Last but not least, we compare eight common missing data imputation baselines: MISGAN [15], rGAIN [43], McFlow [27], OT [23], BRITS [3], GA-GAN [40], GRIN [1], PriSTI [18].

- Statistical learning-based or machine learning-based baselines
 - **Mean**: Mean imputation, which imputes the missing values for each node using the average of the observed values.
 - **KNN** [33]: We calculate the Euclidean distance between each node and select the average of the observations of k -nearest neighbor nodes to impute the missing values.
 - **MissForest** [28]: A tree-based imputation algorithm using the MissForest strategy.
 - **MF** [13]: A method of low rank Matrix decomposition.
 - **MICE** [38]: Impute the missing values using the Multivariate Iterative Chained Equations and multiple imputations.
- Complete traffic data modeling baselines (with pre-filling techniques for imputation task)
 - **STGCN** [44]: Spatio-temporal graph convolution network, which integrates the graph convolution with 1D temporal convolution units.
 - **DCRNN** [16]: Diffusion convolutional recurrent neural network, which integrates the graph convolution with recurrent units.

- **GWNet** [39]: Graph wavenet, which combines the gated TCN and GCN to jointly capture spatio-temporal dependencies.
- **DSTAGNN** [14]: Dynamic spatio-temporal aware graph neural network, which designs an improved multi-head attention mechanism and gated convolution to capture spatio-temporal correlations.
- **D2STGNN** [31]: Decoupled dynamic spatio-temporal graph neural network, which separates the diffusion and inherent information to capture spatio-temporal dependencies.
- Incomplete traffic data imputation baselines
 - **MISGAN** [15]: A GAN-based imputation framework tailored to learn from complex high-dimensional incomplete data.
 - **rGAN** [43]: A GAN-based method with a bidirectional recurrent encoder-decoder.
 - **McFlow** [27]: A deep framework for imputation that leverages normalizing flow generative models and Monte Carlo sampling.
 - **OT** [23]: A deep neural distribution matching method based on optimal transport.
 - **BRITS** [3]: A bidirectional recurrent neural network for missing value imputation in time series data.
 - **GA-GAN** [40]: Graph aggregate generative adversarial network, which combines GraphSAGE [7] and GAN to impute missing values.
 - **GRIN** [1]: Graph recurrent imputation network, which combines recurrent neural network and message-passing neural network.
 - **PriSTI** [18]: A conditional diffusion model for spatio-temporal data imputation, which combines MPNN and conditional diffusion model.

5.1.3 Metrics. In order to verify the performance of our model, we employ the following two metrics to evaluate the imputation of missing values, including Root Mean Square Error (RMSE) and Mean Absolute Percentage Error (MAPE). The formulas are as follows:

$$\text{RMSE}(y, \hat{y}) = \sqrt{\frac{\sum_{i=1}^N (\hat{y}_i - y_i)^2 m_i}{\sum_{i=1}^N m_i}}, \text{MAPE}(y, \hat{y}) = 100\% \times \frac{\sum_{i=1}^N \left| \frac{\hat{y}_i - y_i}{y_i} \right| m_i}{\sum_{i=1}^N m_i}, \quad (18)$$

where y is the ground truth, \hat{y} is the imputed value, and m_i is an element of mask matrix \mathbf{M} .

5.1.4 Implementation. Following the previous works [1, 40], we focus on Completely Missing At Random (MCAR) [17] to simulate the incomplete traffic data. It should be noted that we do not limit other missing patterns. We randomly mask out 50% of the available data. In-depth analysis for different missing ratio are conducted in section 5.5. The number of attention heads in mask-aware spatio-temporal attention is set to 3. Regarding the multi-scale temporal convolution, we use 3 convolution kernels ($K=3, 5, 7$) in METR-LA, and Seattle and PEMS-BAY. We use 2 convolution kernels ($K=3, 5$) in Chengdu and Shenzhen. The learning rate is searched from 10^{-9} to 10^{-2} with a step size 10 and the Adam optimizer is used. We conduct a grid search on each dataset for other major hyperparameters, which is discussed in section 5.6. The model architecture of each baseline is consistent with its original paper. For fairness, we also searched for the optimal hyperparameters of the baselines and selected the best results for comparison. Our implementation is based on torch1.8.0. All experiments are implemented on a server with 2 CPUs (Intel Xeon Silver 4116) and 4 GPUs (NVIDIA GTX 3090).

Table 3. Overall performance on five real-world traffic datasets. We simulate the missing data with a missing ratio $r=0.5$ following the Missing Completely at Random (MCAR) pattern. We run the experiments five times and show the average results. In each column, the **best result** is highlighted in **bold** and the second best is underlined. The marker * indicates that the improvement is statistically significant compared with the best baseline (t-test with p-value < 0.05).

Methods	METR-LA		Seattle		Chengdu		Shenzhen		PEMS-BAY	
	RMSE	MAPE	RMSE	MAPE	RMSE	MAPE	RMSE	MAPE	RMSE	MAPE
Mean	12.69	18.16	7.44	18.76	6.42	22.10	7.07	21.58	5.12	8.68
KNN [33]	7.43	10.31	5.88	10.08	4.60	13.57	4.53	12.03	3.46	4.01
MissForest [28]	6.32	8.47	4.75	8.44	4.16	12.10	4.24	10.69	2.76	3.37
MF [13]	5.75	8.42	4.53	7.94	4.30	13.04	4.65	12.67	2.61	3.23
MICE [38]	6.19	8.97	4.75	8.35	3.96	11.27	3.76	9.65	2.50	3.14
STGCN [44]	7.00	8.95	4.01	6.45	3.48	10.60	3.64	10.52	3.28	3.97
DCRNN [16]	14.75	7.25	3.47	<u>5.24</u>	3.71	10.46	3.50	8.73	2.25	2.22
GWNet [39]	7.50	7.30	4.13	6.29	3.78	10.77	3.60	9.12	2.22	2.14
DSTAGNN [14]	6.38	7.44	3.78	5.91	<u>3.16</u>	9.39	<u>2.94</u>	<u>8.14</u>	1.95	2.03
D2STGNN [31]	14.03	8.08	<u>3.43</u>	5.33	3.20	9.55	2.95	<u>8.14</u>	<u>1.82</u>	2.02
MISGAN [15]	11.97	14.81	6.82	13.63	4.61	15.82	4.49	13.01	5.48	7.04
rGAN [43]	10.36	13.38	6.28	11.60	3.86	12.16	3.72	10.68	4.51	5.69
McFlow [27]	9.50	11.71	5.67	10.55	3.54	10.90	3.37	9.19	4.24	5.16
OT [23]	7.23	10.03	5.35	11.52	4.78	13.75	5.72	13.32	3.59	5.68
BRITS [3]	9.24	11.27	6.15	12.60	4.26	14.12	4.23	12.40	3.00	3.20
GA-GAN [40]	7.15	8.24	4.11	7.39	3.51	10.75	3.26	8.82	2.10	2.18
GRIN [1]	6.24	7.93	4.30	7.56	4.05	12.85	3.47	9.85	2.61	3.03
PriSTI [18]	<u>5.34</u>	<u>6.39</u>	3.96	5.77	3.47	<u>8.95</u>	3.30	8.37	1.80	1.83
MagiNet (ours)	4.96*	6.35*	3.35*	5.10*	2.87*	8.16*	2.74*	7.39*	1.87	<u>1.88</u>

5.2 Overall Performance (RQ1)

The overall performance is shown in Table 3. We make the following observations: (1) MagiNet outperforms other baselines on multiple datasets, yielding an average improvement of 4.31% in RMSE and 3.72% in MAPE, demonstrating the superiority of our method. (2) Complete traffic data modeling methods with pre-filling techniques exhibit unstable performance across different datasets and are inferior to our MagiNet. This deficiency is attributed to their limitations in capturing the inherent spatio-temporal dependencies within incomplete traffic data. In contrast, MagiNet utilizes mask-aware spatio-temporal attention, adaptively adjusting aggregation coefficients based on observation information, which extracts the intrinsic dependencies and alleviates the over-smoothing effect. Consequently, MagiNet surpasses these complete traffic data modeling methods with pre-filling techniques, demonstrating an average performance enhancement of 7.56% and 8.87% in RMSE and MAPE, respectively. (3) MagiNet significantly outperforms existing missing data imputation methods, as these methods rely on pre-filling techniques to initialize missing values, introducing uncontrollable noise and resulting in error propagation. Instead, MagiNet adopts the learnable missing encoding approach to represent missing values, avoiding noise introduction. (4) PriSTI performs slightly better than MagiNet on PEMS-BAY dataset, potentially attributed to PriSTI's imputation of missing values through a substantial number of generation steps, making it more suitable for datasets with low variance such as PEMS-BAY. However, MagiNet consistently

Table 4. Ablation study of MagiNet on five datasets. We run the experiments five times and show the average results. The marker * indicates that the improvement is statistically significant compared with the best baseline (t-test with p-value < 0.05).

Method	METR-LA		Seattle		Chengdu		Shenzhen		PEMS-BAY	
	RMSE	MAPE	RMSE	MAPE	RMSE	MAPE	RMSE	MAPE	RMSE	MAPE
zero prefill	5.05	6.57	3.42	5.27	2.99	8.56	2.82	7.70	1.90	1.91
mean prefill	5.08	6.49	3.40	5.22	3.11	9.12	2.80	7.65	1.89	1.91
w/o AMSTenc	5.19	6.46	3.45	5.29	3.56	10.07	3.47	8.76	1.91	1.92
w/o MASTatt	4.99	6.45	3.36	5.11	3.28	9.52	2.88	7.87	1.89	1.91
w/o Graphconv	7.14	7.12	3.96	6.07	3.37	9.83	3.00	8.18	1.93	1.93
w/o GTconv	5.06	6.43	3.40	5.23	2.97	8.52	2.79	7.58	1.88	1.90
w/o MASTdec	6.94	7.50	4.01	6.12	3.37	9.79	2.99	8.10	2.02	2.07
MagiNet	4.96*	6.35*	3.35*	5.10*	2.87*	8.16*	2.74*	7.39*	1.88	1.89*

demonstrates strong performance across other datasets. Further experiments about the effectiveness of our MagiNet are shown in section 5.3 and section 5.4.

5.3 Ablation Study (RQ2)

To verify the effectiveness of each component of MagiNet, we systematically modify or remove individual components to create variants of MagiNet and do grid search to optimize the performance of these variants. Seven types of MagiNet variants are considered. We set (1) *zero prefill* and (2) *mean prefill* to assess the performance of pre-filling missing values with zero and mean values, respectively. (3) We set *w/o AMSTenc* to test the performance of replacing the adaptive mask spatio-temporal encoder (*AMSTenc*) with a regular embedding layer. (4) We set *w/o MASTatt* to test the performance of MagiNet without mask-aware spatio-temporal attention (*MASTatt*) mechanism. (5) We set *w/o Graphconv* to test the performance of MagiNet without attention-based graph convolution (*Graphconv*). (6) We set *w/o GTconv* to test the performance of MagiNet without multi-scale gated temporal convolution (*GTconv*). (7) We set *w/o MASTdec* to test the performance of replacing the mask-aware spatio-temporal decoder (*MASTdec*) with a single regression layer.

As shown in Table 4, MagiNet outperforms other variants across five datasets. The superior performance of MagiNet over *zero prefill* and *mean prefill* indicates the positive impact of learnable missing encoding. Moreover, MagiNet is superior to *w/o AMSTenc*, suggesting that the adaptive mask spatio-temporal encoder plays a vital role in learning the representation of incomplete traffic data. MagiNet surpasses *w/o MASTatt*, highlighting the positive role of mask-aware spatio-temporal attention. MagiNet also surpasses *w/o Graphconv* and *w/o GTconv*, which indicates that the attention-based graph convolution and multi-scale gated temporal convolution modules are also important to aggregate information. Furthermore, MagiNet significantly outperforms *w/o MASTdec*, showing the significance of capturing inherent spatio-temporal correlations.

5.4 Case Study (RQ2)

To intuitively understand how MagiNet imputes the incomplete traffic data, we visualize the imputation curves between MagiNet and its variants on two datasets with high variance, Seattle and METR-LA. Specifically, we randomly select two snapshots of imputation results: node #2 in Seattle and node #85 in METR-LA. As shown in Figure 3, MagiNet outperforms *mean prefill* and *w/o MASTatt*, especially in continuous missing positions and dynamic positions, such as time step

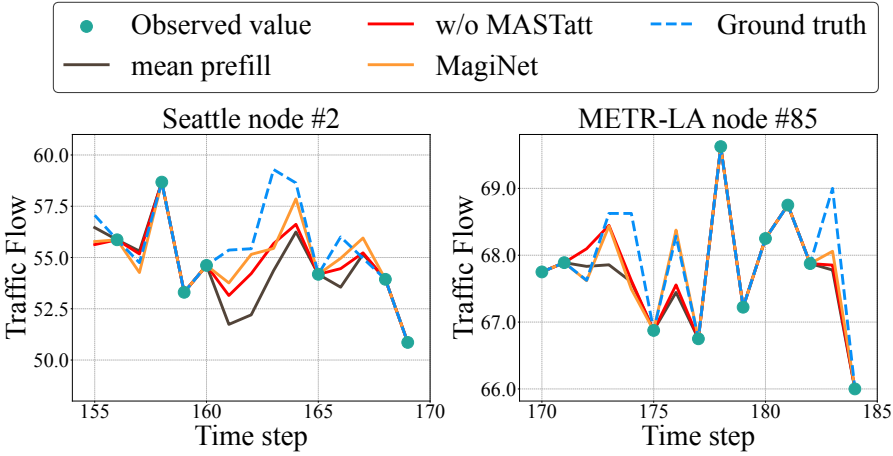


Fig. 3. Comparison of imputation curves between MagiNet and its variants for two snapshots: node #2 in Seattle and node #85 in METR-LA.

160 to 168 in Seattle and time step 171 to 176 in METR-LA. The capability of MagiNet to mitigate imputation errors can be attributed to *AMSTenc*, which substitutes pre-filling techniques and avoids introducing noise, and *MASTatt*, designed to capture inherent spatio-temporal dependencies within incomplete traffic data.

5.5 Sensitivity Analysis (RQ3)

We carry out an assessment of performance consistency with respect to different missing ratios. We present the results on METR-LA, Seattle, Chengdu, and Shenzhen datasets. To take into account comprehensively of the sufficiency and sparsity of missing data, we select the missing ratio r from 20% to 70%. This is because when the missing ratio is too low, the model may simply use the values near the missing points for interpolation. Conversely, when the missing ratio is too high, there is little valuable information, resulting in rapidly deterioration in model performance. Then, we select five representative models from the baselines: MICE [38], GA-GAN [40], GRIN [1], and DSTAGNN [14], PriSTI [18] to compare with MagiNet. The results are shown in Figure 4. The imputation performance degrades as the missing ratio increases, aligning with our intuition. MagiNet consistently performs as the best, with the lowest degradation speed, suggesting that MagiNet demonstrates the capability to maintain remarkable consistency across various missing ratios.

5.6 Hyperparameter Study (RQ4)

We determine the hyperparameters by analyzing the experimental results as illustrated in Figure 5. (1) We vary the size of hidden dimension of incomplete traffic data h from 16 to 128, which impacts the model's capability to capture inherent features. Overall, the optimal performance can be achieved when $h = 16$. Small h is insufficient for learning incomplete traffic data representation, while large h is prone to overfitting. (2) We vary the number of spatio-temporal blocks s ranging from 1 to 5, which directly influences the extent of intrinsic spatio-temporal correlations extracted by the model. When s is small, the spatio-temporal correlation capturing is insufficient, while s is large, the model overfits some outliers, leading to a decrease in performance. (3) We adjust the

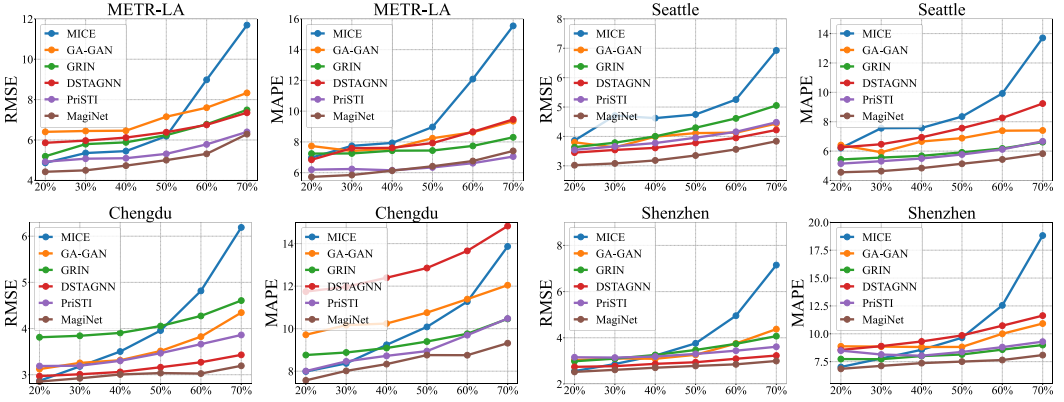


Fig. 4. Sensitivity analysis on METR-LA, Seattle, Chengdu, and Shenzhen datasets with respect to different missing ratio r from 20% to 70%.

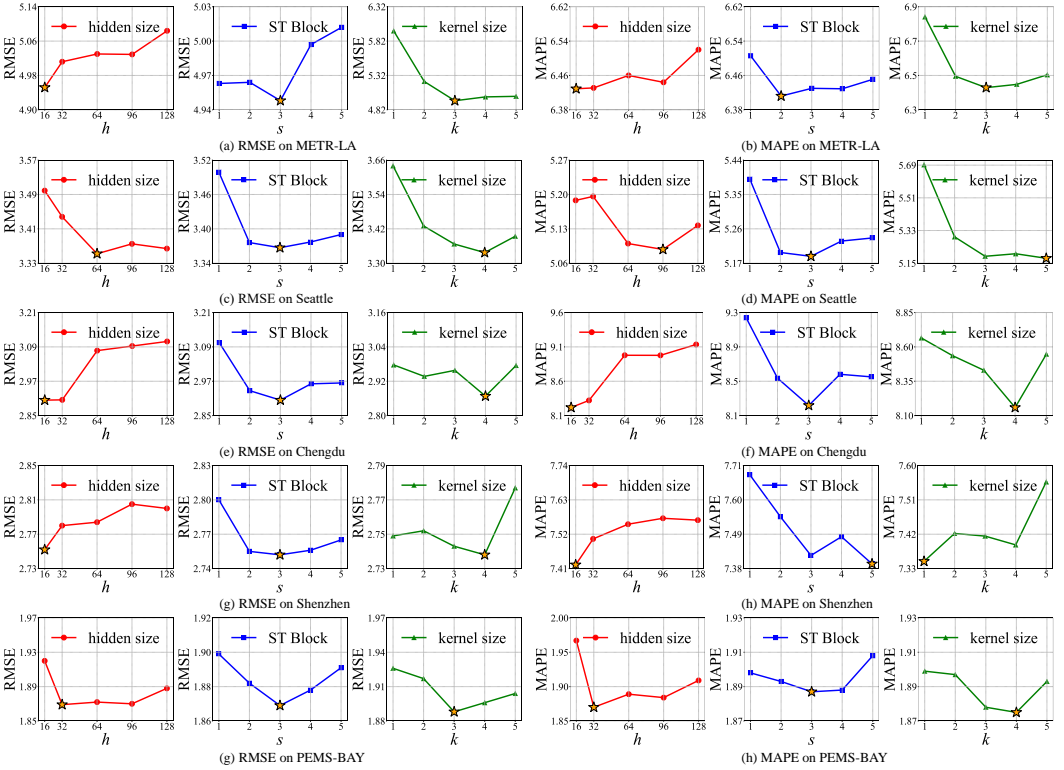


Fig. 5. Hyperparameter study on three key parameters of MagiNet: hidden size h , spatio-temporal blocks s , mask-aware spatial kernel size k .

size of spatial convolution kernel k between 1 and 5, which determines the range of aggregated neighbor information. Setting $k = 3$ or $k = 4$ often yields better performance.

5.7 Visualization Results

To further intuitively understand the imputation performance of our model MagiNet, we provide more visualization of incomplete traffic data imputation results on five datasets, as shown in Figure 6 and Figure 7. We randomly select two nodes from each dataset to demonstrate the imputation and ground truth within a single day.

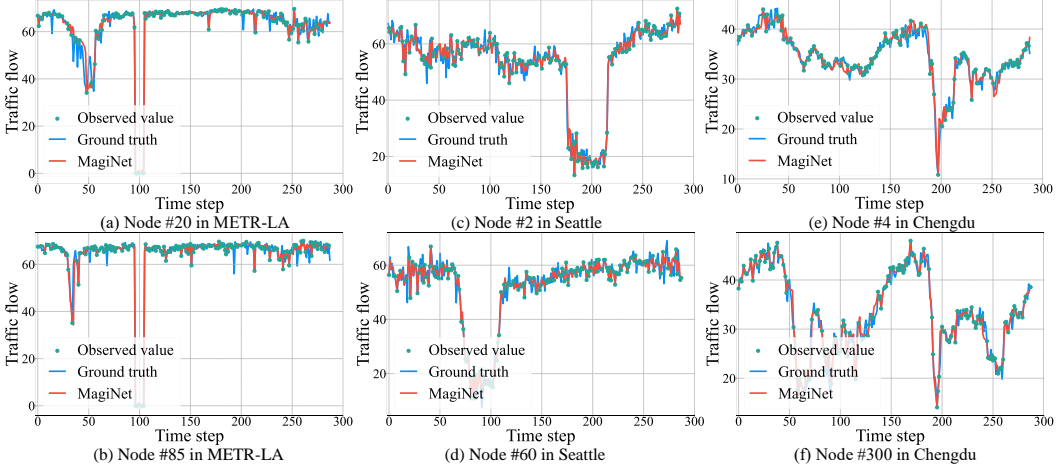


Fig. 6. Imputation results of incomplete traffic data in METR-LA, Seattle, and Chengdu.

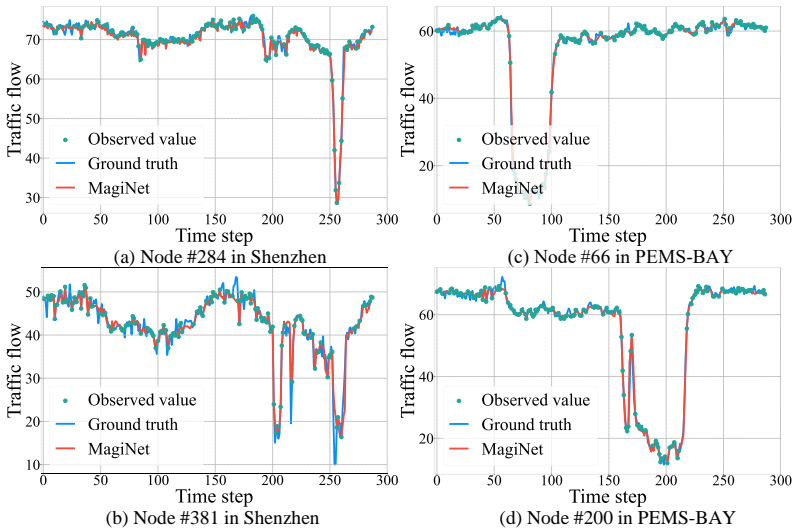


Fig. 7. Imputation results of incomplete traffic data in Shenzhen and PEMS-BAY.

6 CONCLUSION

In this paper, we propose MagiNet, a mask-aware graph imputation network to impute missing values within incomplete traffic data. MagiNet employs an adaptive mask spatio-temporal encoder

to represent the incomplete traffic data and a mask-aware spatio-temporal decoder that stacks multiple blocks to capture inherent spatio-temporal dependencies in the presence of missing values. Experimental results demonstrate that our MagiNet achieves outstanding performance across five public datasets for incomplete traffic data imputation task. In the future, we intend to extend our MagiNet to address probabilistic imputation task and explore its scalability on larger scale traffic dataset.

REFERENCES

- [1] Cini Andrea, Marisca Ivan, Cesare Alippi, et al. 2022. Filling the G_ap_s: Multivariate Time Series Imputation by Graph Neural Networks. In *ICLR 2022*. 1–20.
- [2] Shuqin Cao, Libing Wu, Jia Wu, Dan Wu, and Qingan Li. 2022. A spatio-temporal sequence-to-sequence network for traffic flow prediction. *Information Sciences* 610 (2022), 185–203.
- [3] Wei Cao, Dong Wang, Jian Li, Hao Zhou, Lei Li, and Yitan Li. 2018. Brits: Bidirectional recurrent imputation for time series. *Advances in neural information processing systems* 31 (2018).
- [4] Jicong Fan. 2022. Dynamic nonlinear matrix completion for time-varying data imputation. In *Proceedings of the AAAI Conference on Artificial Intelligence*, Vol. 36. 6587–6596.
- [5] Yongshun Gong, Zhibin Li, Jian Zhang, Wei Liu, Yilong Yin, and Yu Zheng. 2021. Missing value imputation for multi-view urban statistical data via spatial correlation learning. *IEEE Transactions on Knowledge and Data Engineering* 35, 1 (2021), 686–698.
- [6] Ian Goodfellow, Jean Pouget-Abadie, Mehdi Mirza, Bing Xu, David Warde-Farley, Sherjil Ozair, Aaron Courville, and Yoshua Bengio. 2020. Generative adversarial networks. *Commun. ACM* 63, 11 (2020), 139–144.
- [7] Will Hamilton, Zhitao Ying, and Jure Leskovec. 2017. Inductive representation learning on large graphs. *Advances in neural information processing systems* 30 (2017).
- [8] Liangzhe Han, Bowen Du, Leilei Sun, Yanjie Fu, Yisheng Lv, and Hui Xiong. 2021. Dynamic and multi-faceted spatio-temporal deep learning for traffic speed forecasting. In *Proceedings of the 27th ACM SIGKDD conference on knowledge discovery & data mining*. 547–555.
- [9] Haixu He, Jining Yan, Lizhe Wang, Dong Liang, Jianyi Peng, and Chengjun Li. 2022. Bayesian temporal tensor factorization-based interpolation for time-series remote sensing data with large-area missing observations. *IEEE Transactions on Geoscience and Remote Sensing* 60 (2022), 1–13.
- [10] Xiaoyi Jia, Xiaoyu Dong, Meng Chen, and Xiaohui Yu. 2021. Missing data imputation for traffic congestion data based on joint matrix factorization. *Knowledge-Based Systems* 225 (2021), 107114.
- [11] Durk P Kingma and Prafulla Dhariwal. 2018. Glow: Generative flow with invertible 1x1 convolutions. *Advances in neural information processing systems* 31 (2018).
- [12] Diederik P Kingma and Max Welling. 2013. Auto-encoding variational bayes. *arXiv preprint arXiv:1312.6114* (2013).
- [13] Linghe Kong, Mingyuan Xia, Xiao-Yang Liu, Guangshuo Chen, Yu Gu, Min-You Wu, and Xue Liu. 2013. Data loss and reconstruction in wireless sensor networks. *IEEE Transactions on Parallel and Distributed Systems* 25, 11 (2013), 2818–2828.
- [14] Shiyong Lan, Yitong Ma, Weikang Huang, Wenwu Wang, Hongyu Yang, and Pyang Li. 2022. Dstagnn: Dynamic spatial-temporal aware graph neural network for traffic flow forecasting. In *International conference on machine learning*. PMLR, 11906–11917.
- [15] Steven Cheng-Xian Li, Bo Jiang, and Benjamin Marlin. 2019. Misgan: Learning from incomplete data with generative adversarial networks. *arXiv preprint arXiv:1902.09599* (2019).
- [16] Yaguang Li, Rose Yu, Cyrus Shahabi, and Yan Liu. 2017. Diffusion convolutional recurrent neural network: Data-driven traffic forecasting. *arXiv preprint arXiv:1707.01926* (2017).
- [17] Roderick JA Little and Donald B Rubin. 2019. *Statistical analysis with missing data*. Vol. 793. John Wiley & Sons.
- [18] Mingzhe Liu, Han Huang, Hao Feng, Leilei Sun, Bowen Du, and Yanjie Fu. 2023. PriSTI: A Conditional Diffusion Framework for Spatiotemporal Imputation. *arXiv preprint arXiv:2302.09746* (2023).
- [19] Bin Lu, Xiaoying Gan, Haiming Jin, Luoyi Fu, and Haisong Zhang. 2020. Spatiotemporal adaptive gated graph convolution network for urban traffic flow forecasting. In *Proceedings of the 29th ACM International conference on information & knowledge management*. 1025–1034.
- [20] Bin Lu, Xiaoying Gan, Weinan Zhang, Huaxiu Yao, Luoyi Fu, and Xinbing Wang. 2022. Spatio-Temporal Graph Few-Shot Learning with Cross-City Knowledge Transfer. In *Proceedings of the 28th ACM SIGKDD Conference on Knowledge Discovery and Data Mining*. 1162–1172.
- [21] Pierre-Alexandre Mattei and Jes Frellsen. 2019. MIWAE: Deep generative modelling and imputation of incomplete data sets. In *International conference on machine learning*. PMLR, 4413–4423.

- [22] Ardalan Mirzaei, Stephen R Carter, Asad E Patanwala, and Carl R Schneider. 2022. Missing data in surveys: Key concepts, approaches, and applications. *Research in Social and Administrative Pharmacy* 18, 2 (2022), 2308–2316.
- [23] Boris Muzellec, Julie Josse, Claire Boyer, and Marco Cuturi. 2020. Missing data imputation using optimal transport. In *International Conference on Machine Learning*. PMLR, 7130–7140.
- [24] Huiling Qin, Xianyuan Zhan, Yuanxun Li, Xiaodu Yang, and Yu Zheng. 2021. Network-wide traffic states imputation using self-interested coalitional learning. In *Proceedings of the 27th ACM SIGKDD Conference on Knowledge Discovery & Data Mining*. 1370–1378.
- [25] Huiling Qin, Xianyuan Zhan, Yuanxun Li, Xiaodu Yang, and Yu Zheng. 2021. Network-wide traffic states imputation using self-interested coalitional learning. In *Proceedings of the 27th ACM SIGKDD Conference on Knowledge Discovery & Data Mining*. 1370–1378.
- [26] Li Qu, Li Li, Yi Zhang, and Jianming Hu. 2009. PPCA-based missing data imputation for traffic flow volume: A systematical approach. *IEEE Transactions on intelligent transportation systems* 10, 3 (2009), 512–522.
- [27] Trevor W Richardson, Wencheng Wu, Lei Lin, Beilei Xu, and Edgar A Bernal. 2020. Mcflow: Monte carlo flow models for data imputation. In *Proceedings of the IEEE/CVF Conference on Computer Vision and Pattern Recognition*. 14205–14214.
- [28] Alex Rubinsteyn and Sergey Feldman. [n. d.]. *fancyimpute: An Imputation Library for Python*. <https://github.com/iskandr/fancyimpute>
- [29] Koustuv Saha, Manikanta D Reddy, Vedant das Swain, Julie M Gregg, Ted Grover, Suwen Lin, Gonzalo J Martinez, Stephen M Mattingly, Shayan Mirjafari, Raghu Mulukutla, et al. 2019. Imputing missing social media data stream in multisensor studies of human behavior. In *2019 8th International Conference on Affective Computing and Intelligent Interaction (ACII)*. IEEE, 178–184.
- [30] Zezhi Shao, Zhao Zhang, Fei Wang, and Yongjun Xu. 2022. Pre-training enhanced spatial-temporal graph neural network for multivariate time series forecasting. In *Proceedings of the 28th ACM SIGKDD Conference on Knowledge Discovery and Data Mining*. 1567–1577.
- [31] Zezhi Shao, Zhao Zhang, Wei Wei, Fei Wang, Yongjun Xu, Xin Cao, and Christian S Jensen. 2022. Decoupled dynamic spatial-temporal graph neural network for traffic forecasting. *Proceedings of the VLDB Endowment* 15, 11 (2022), 2733–2746.
- [32] Martin Simonovsky and Nikos Komodakis. 2017. Dynamic edge-conditioned filters in convolutional neural networks on graphs. In *Proceedings of the IEEE conference on computer vision and pattern recognition*. 3693–3702.
- [33] Shaoxu Song, Chunping Li, and Xiaoquan Zhang. 2015. Turn waste into wealth: On simultaneous clustering and cleaning over dirty data. In *Proceedings of the 21th ACM SIGKDD International Conference on Knowledge Discovery and Data Mining*. 1115–1124.
- [34] Ashish Vaswani, Noam Shazeer, Niki Parmar, Jakob Uszkoreit, Llion Jones, Aidan N Gomez, Łukasz Kaiser, and Illia Polosukhin. 2017. Attention is all you need. *Advances in neural information processing systems* 30 (2017).
- [35] Ao Wang, Yongchao Ye, Xiaozhuang Song, Shiyao Zhang, and JQ James. 2023. Traffic Prediction With Missing Data: A Multi-Task Learning Approach. *IEEE Transactions on Intelligent Transportation Systems* 24, 4 (2023), 4189–4202.
- [36] Xiaoyang Wang, Yao Ma, Yiqi Wang, Wei Jin, Xin Wang, Jiliang Tang, Caiyan Jia, and Jian Yu. 2020. Traffic flow prediction via spatial temporal graph neural network. In *Proceedings of the web conference 2020*. 1082–1092.
- [37] Ziyuan Wang, Hoang Tam Vo, Mahsa Salehi, Laura Irina Rusu, Claire Reeves, and Anna Phan. 2017. A large-scale spatio-temporal data analytics system for wildfire risk management. In *Proceedings of the Fourth International ACM Workshop on Managing and Mining Enriched Geo-Spatial Data*. 1–6.
- [38] Ian R White, Patrick Royston, and Angela M Wood. 2011. Multiple imputation using chained equations: issues and guidance for practice. *Statistics in medicine* 30, 4 (2011), 377–399.
- [39] Zonghan Wu, Shirui Pan, Guodong Long, Jing Jiang, and Chengqi Zhang. 2019. Graph wavenet for deep spatial-temporal graph modeling. *arXiv preprint arXiv:1906.00121* (2019).
- [40] Dongwei Xu, Hang Peng, Chenchen Wei, Xuetian Shang, and Haijian Li. 2022. Traffic State Data Imputation: An Efficient Generating Method Based on the Graph Aggregator. *IEEE Transactions on Intelligent Transportation Systems* 23, 8 (2022).
- [41] Yi Xu, Armin Bazarjani, Hyung-gun Chi, Chiho Choi, and Yun Fu. 2023. Uncovering the missing pattern: Unified framework towards trajectory imputation and prediction. In *Proceedings of the IEEE/CVF Conference on Computer Vision and Pattern Recognition*. 9632–9643.
- [42] Xiuwen Yi, Zhewen Duan, Ting Li, Tianrui Li, Junbo Zhang, and Yu Zheng. 2019. Citytraffic: Modeling citywide traffic via neural memorization and generalization approach. In *Proceedings of the 28th ACM international conference on information and knowledge management*. 2665–2671.
- [43] Jinsung Yoon, James Jordon, and Mihaela Schaar. 2018. Gain: Missing data imputation using generative adversarial nets. In *International conference on machine learning*. PMLR, 5689–5698.
- [44] Bing Yu, Haoteng Yin, and Zhanxing Zhu. 2017. Spatio-temporal graph convolutional networks: A deep learning framework for traffic forecasting. *arXiv preprint arXiv:1709.04875* (2017).

- [45] Yingxue Zhang, Yanhua Li, Xun Zhou, Xiangnan Kong, and Jun Luo. 2020. Curb-gan: Conditional urban traffic estimation through spatio-temporal generative adversarial networks. In *Proceedings of the 26th ACM SIGKDD International Conference on Knowledge Discovery & Data Mining*. 842–852.
- [46] Zimu Zheng, Dan Wang, Jian Pei, Yi Yuan, Cheng Fan, and Fu Xiao. 2016. Urban traffic prediction through the second use of inexpensive big data from buildings. In *Proceedings of the 25th ACM International on Conference on Information and Knowledge Management*. 1363–1372.

Received 20 February 2007; revised 12 March 2009; accepted 5 June 2009